SPANDIDOS PUBLICATIONS

INTERNATIONAL JOURNAL OF MOLECULAR MEDICINE 44: 1436-1446, 2019

Next-generation sequencing predicts interaction network between miRNA and target genes in lipoteichoic acid-stimulated human neutrophils

MENG-CHI YEN[1,2], I-JENG YEH[1,2], KUAN-TING LIU[1-3], SHU-FANG JIAN[2], CHIA-JUNG LIN[2,4], MING-JU TSAI[2,3,5,6] and PO-LIN KUO[2,7,8]

[1]Department of Emergency Medicine, Kaohsiung Medical University Hospital; [2]Graduate Institute of Clinical Medicine; [3]School of Medicine, College of Medicine, Kaohsiung Medical University; [4]Division of Trauma and Surgical Critical Care, Department of Surgery; [5]Division of Pulmonary and Critical Care Medicine, Department of Internal Medicine, Kaohsiung Medical University Hospital; [6]Department of Respiratory Therapy, College of Medicine; [7]Center for Cancer Research, Kaohsiung Medical University, Kaohsiung 807; [8]Institute of Medical Science and Technology, National Sun Yat-Sen University, Kaohsiung 804, Taiwan, R.O.C.

Received April 4, 2019; Accepted June 28, 2019

DOI: 10.3892/ijmm.2019.4295

Abstract. Toll-like receptors (TLRs), which are a class of pattern-recognition receptors, can sense specific molecules of pathogens and then activate immune cells, such as neutrophils. The regulation of TLR signaling in immune cells has been investigated by various studies. However, the interaction of TLR signaling-activated microRNAs (miRNAs) and genes has not been well investigated in a specific type of immune cells. In the present study, neutrophils were isolated from peripheral blood of a healthy donor, and then treated for 16 h with *Staphylococcus aureus* lipoteichoic acid (LTA), which is an agonist of TLR2. The miRNA and mRNA expression profiles were analyzed via next-generation sequencing and bioinformatics approaches. A total of 290 differentially expressed genes between LTA-treated and vehicle-treated neutrophils were identified. Gene ontology analysis revealed that various biological processes and pathways, including inflammatory responses, defense response, positive regulation of cell migration, motility, and locomotion, and cell surface receptor signaling pathway, were significantly enriched. In addition, 38 differentially expressed miRNAs were identified and predicted to be involved in regulating signal transduction and cell communication. The interaction of 4 miRNAs (hsa-miR-34a-5p, hsa-miR-34c-5p, hsa-miR-708-5p, and hsa-miR-1271-5p) and 5 genes (MET, CACNB3, TNS3, TTYH3, and HBEGF) was proposed to participate in the LTA-induced signaling network. The present findings may provide novel information for understanding the detailed expression profiles and potential networks between miRNAs and their target genes in LTA-stimulated healthy neutrophils.

Correspondence to: Dr Ming-Ju Tsai, School of Medicine, College of Medicine, Kaohsiung Medical University, 100 Shih-Chuan 1st Road, Kaohsiung 807, Taiwan, R.O.C.
E-mail: siegfriedtsai@gmail.com

Key words: neutrophil, lipoteichoic acid, microRNA, innate immunity

Introduction

The innate immune system can detect the presence of pathogens, such as viruses and bacteria, and activate immune responses to eliminate the infections. These pathogens can be recognized by pattern-recognition receptors (PRRs) and trigger activation of innate immunity (1,2). The family of Toll-like receptors (TLRs) is a class of PRRs in mammals (3). TLR4 is an important receptor recognizing lipopolysaccharide (LPS), which is a component of the outer membrane of Gram-negative bacteria (4,5). By contrast, the wall components of Gram-positive bacteria, such as peptidoglycan (PGN) and lipoteichoic acid (LTA), are recognized by TLR2 (6-8). PGN and LTA can induce septic shock and multiple organ failure (9).

TLR2 expression can be detected in various types of human immune cells, including monocytes, macrophages, dendritic cells and polymorphonuclear leukocytes (also termed granulocytes and include neutrophils, basophils and eosinophils) (10). In peripheral blood, neutrophils are the most abundant type of granulocytes and the first r immune cells to respond to infections. When human neutrophils are exposed to LTA, cell migration, degranulation, secretion of pro-inflammatory factors [including interleukin (IL)-8, tumor necrosis factor-α (TNF-α) and granulocyte colony-stimulating factor (G-CSF)], increased production of reactive oxygen species (ROS) and antimicrobial activity, and activation of TLR2 and NF-κB-mediated signaling pathways have been reported (11-14).

MicroRNA (miRNA) is a group of small non-coding RNAs with ~22 nucleotides. Emerging evidence suggests that

miRNAs are involved in regulation of gene expression and immune responses (15,16). For example, miR-155, miR-146a, miR-UL112-3p and miR-344b-1-3p have been demonstrated to interact with TLR2 in pathological conditions (17-21). However, the interaction of miRNA and LTA-mediated immune activation has not been extensively investigated in a specific type of immune cells. Thus, the present study aimed to investigate the expression mRNA and miRNA in *Staphylococcus aureus* LTA-stimulated human neutrophils via next-generation sequencing. To understand the LTA-mediated effect in healthy immune cells, neutrophils were obtained from the peripheral blood of a healthy donor.

Materials and methods

Neutrophil isolation and LTA treatment. The present study was approved by the Institutional Review Board of Kaohsiung Medical University Hospital (IRB no. KMUH-IRB-20120287). A total of 10 ml venous blood was obtained from a healthy donor. The participant agreed to the use of their sample in research and signed informed consent during the period Jan 2013 to Jan 2014. Human neutrophils were separated from whole blood using CD66abce microbeads (Miltenyi Biotec GbmH), according to manufacturer's instruction. Subsequently, $3x10^7$ isolated neutrophils were cultured in RPMI1640 medium containing 10% fetal bovine serum, 100 U/ml penicillin G, 100 μg/ml streptomycin and 0.25 μg/ml amphotericin B (Thermo Fisher Scientific, Inc.), and 1 μg/ml of LTA (from *S. aureus*; LTA group; cat. no. L2515; Sigma-Aldrich; Merck KgaA) or double distilled water (vehicle group) in 5% CO_2 air atmosphere at 37˚C for 16 h. Neutrophils were collected for RNA isolation. The purity of isolated CD66abce$^+$ cells was evaluated via flow cytometry. Cells were stained with Alexa Fluor 647-conjugated anti-human CD66b (1:20; cat. no. 561645; BD Pharmingen), according to manufacturer's instructions. The cells were then washed and analyzed using a BD Accuri C6 flow cytometer with BD Accuri C6 software version 1.0.264.21 (BD Biosciences).

RNA isolation. Total RNA was extracted using TRIzol® reagent (Thermo Fisher Scientific, Inc.) according to the supplier's protocol. Purified RNA was quantified using a ND-1000 spectrophotometer (NanoDrop Technologies; Thermo Fisher Scientific, Inc.) and the quality was confirmed using an Agilent 2100 Bioanalyzer and an RNA 6000 Pico LabChip RNA (Agilent Technologies, Inc.). The RNA integrity number (RIN) resulting from the Agilent Bioanalyzer was 8.3 for the LTA-stimulated cells and 7.6 for the vehicle-stimulated cells. The quality report is shown in Fig. S1.

Library preparation, sequencing, alignment and differential expression analysis. Sequencing for mRNA and miRNA was commercially performed by Welgene Biotech Co., Ltd. All RNA sample preparation procedures were carried out according to the official Illumina protocol (Illumina, Inc.). For mRNA sequencing, Agilent's SureSelect Strand-Specific RNA Library Preparation kit (Agilent Technologies, Inc.) was used for library construction, followed by AMPure XP Beads (Agilent Technologies, Inc.) size selection. The sequence was directly determined via Illumina's sequencing-by-synthesis technology. Sequencing data were generated by Welgene's pipeline based on Illumina's base-calling program bcl2fastq v2.2.0. For miRNA sequencing, samples were prepared using the TruSeq™ miRNA Library kit (Illumina, Inc.), following the supplier's guide. Libraries were sequenced on an Illumina instrument (75-cycle single-end read; 75SE) and miRNA sequencing data was processed using the Illumina software BCL2FASTQ v2.20. Sequence Quality Trimming, performed by Trimmomatic version 0.36 (22). HISAT2 was used for mRNA alignment (23) and miRDeep2 was used for miRNA alignment (24). The expression levels were normalized by calculating fragments per kilobase of transcript per million mapped reads (FPKM). Differential expression analysis was performed via Cuffdiff (Cufflinks 2.2.1) (25). P-value was calculated by Cuffdiff with non-grouped sample using the 'blind' method, in which all samples are treated as replicates of a single global 'condition' and used to build one model (25).

Reverse transcription-quantitative PCR (RT-qPCR). Isolated cells ($5x10^5$) were seeded into several wells of a 24-well plate and treated with vehicle or 1 μg/ml LTA for 16 h. Total RNA was isolated using TRIzol reagent (Thermo Fisher Scientific, Inc.). Equal amount of total RNA was reverse transcribed via the PrimeScript RT reagent kit (Clontech Laboratories, Inc.). qPCR was performed with SYBR-Green Master Mix (Applied Biosystems; Thermo Fisher Scientific, Inc.) on a Real-Time PCR system (QuantStudio 3D Digital PCR System; Thermo Fisher Scientific, Inc.). The thermocycling conditions were: 20 sec at 95˚C, followed by 40 amplification cycles of 95˚C for 3 sec and 60˚C for 30 sec. The primers were as follows: Human chemokine (C-C motif) ligand (CCL) 2, forward 5'-TCTGTG CCTGCTGCTCATAG-3' and reverse 5'-TGGAATCCTGAA CCCACTTC-3'; human CCL7, forward 5'-ACCACCAGTAGC CACTGTCC-3' and reverse 5'-TTGGGTTTTCTTGTCCAG GT-3'; human C-X-C motif chemokine ligand 5 (CXCL5), forward 5'-TGTTTACAGACCACGCAAGG-3' and reverse 5'-GGGGCTTCTGGATCAAGAC-3'; and human GAPDH, forward 5'-GAGTCAACGGATTTGGTCGT-3' and reverse 5'-TTGATTTTGGAGGGATCTCG-3'. The relative mRNA expression levels were normalized to the GAPDH expression and calculated using the $2^{-\Delta\Delta Cq}$ method (26).

Gene ontology (GO) analysis of genes and miRNAs. The criteria of differential mRNA expression were set at fold change ≥2.0, FPKM >0.8 and P-value <0.05. For determining the function of LTA-affected genes, the biological process of GO (GOTERM_BP_ALL) analysis and Kyoto encyclopedia of genes and genomes (KEGG) pathway analysis were performed via DAVID Bioinformatics Resources 6.8 (https://david.ncifcrf.gov/home.jsp) (27,28). In addition, gene set enrichment analysis (GSEA; http://www.broad.mit.edu/gsea/) (29,30) was performed using the GO biological processes database c5.bp.v6.2. The criteria of differential miRNA expression were set at fold change ≥2.0 and reads per million (RPM) >1. GO analysis of miRNA was performed via the GSEA method of miRNA Enrichment Analysis and Annotation Tool (miEAA; https://ccb-compute2.cs.uni-saarland.de/mieaa_tool/) (31).

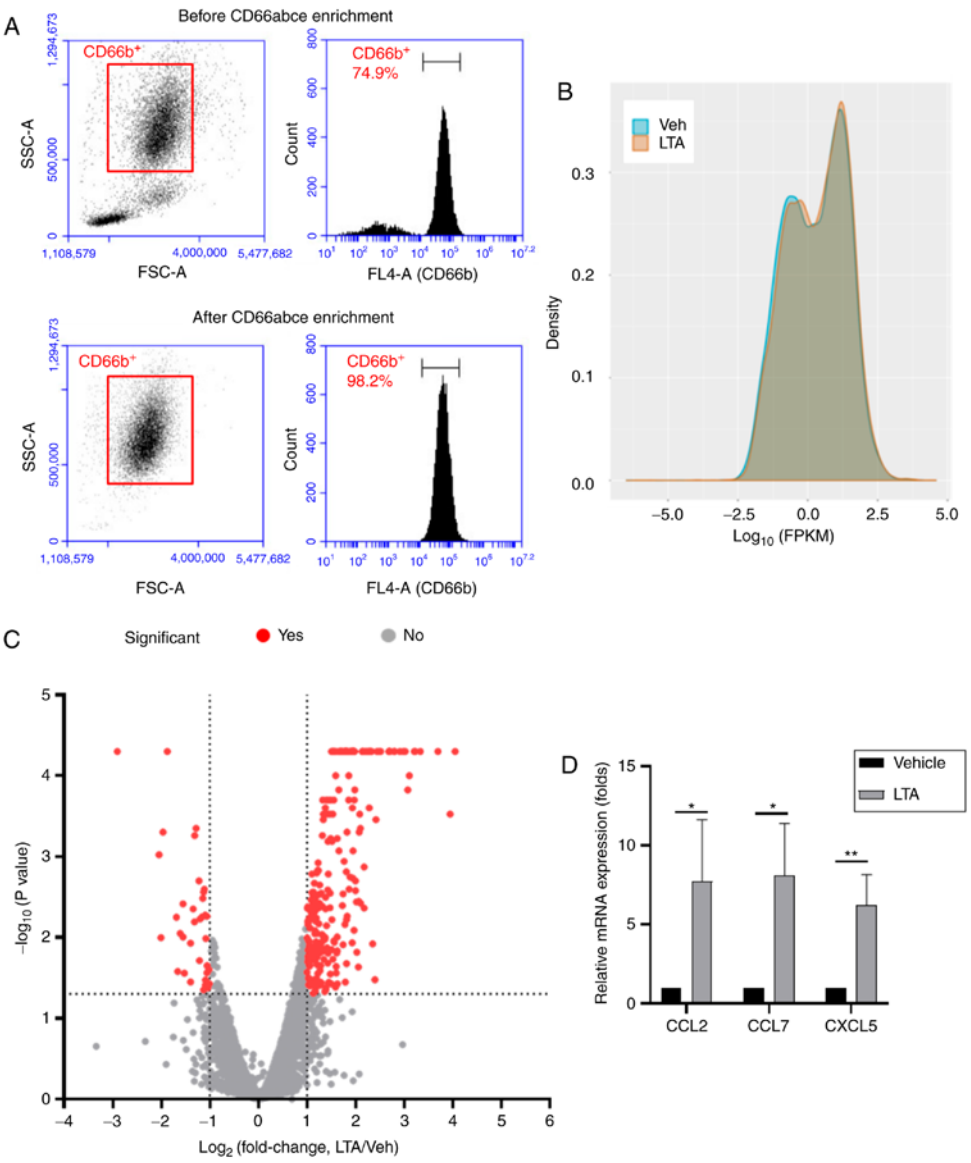

Figure 1. Distribution of mRNA expression in LTA and vehicle-stimulated neutrophils. (A) Purity of enriched human CD66abce+ cells. Upper panel and lower panel reveal the total cell population (left) and the CD66b expression (right) before and after CD66abce enrichment, respectively. (B) Density plot of the distributions of FPKM scores across the two samples. (C) Volcano plot (log_2 fold-change vs. log_{10} P-value) of upregulated and downregulated genes shows the differential mRNA distribution for the sample pair. The dash line indicated the criteria of significant genes. (D) Reverse transcription-qPCR analysis of the CCL2, CCL7 and CXCL5 mRNA expression levels. Data are presented as the mean ± standard deviation. Three replicates were performed. *P<0.05 and **P<0.01 vs. vehicle group. LTA, lipoteichoic acid; FPKM, fragments per kilobase of transcript per million; FSC, forward scatter; SSC, side scatter; Veh, vehicle.

Interaction between miRNA and mRNA. To predict the miRNA-targeted mRNAs, the Funrich software version 3.1.3 (32) and miRDB 6.0 (miRNAs with Target Score >90 were selected) were used (33). The miRNA target genes were determined using two databases: TargetScan 7.2 (http://www.targetscan.org/vert_72/) (34) and miRTarBase 7.0 (http://mirtarbase.mbc.nctu.edu.tw/php/index.php) (35). The network was drawn by using stringApp 1.4.1 plugin in Cytoscape software 3.7.1 (36,37).

Statistical analysis. The Venn diagram was drawn via the website http://bioinformatics.psb.ugent.be/webtools/Venn/, accessed on 22 January 2019. The statistical analysis associated with the Venn diagram was performed via the website http://nemates.org/MA/progs/overlap_stats.html. The number of genes in the genome was set to 1,917 miRNAs according to the latest information of miRBase. For GSEA, P-values <0.01 and false discovery rate (FDR) <25% were considered significant. For GSEA of miRNAs P-values <0.05 were considered significant. All other graphs were produced in GraphPad Prism 8 software (GraphPad Software, Inc.). The Student's t-test was used for analysis of differences between the vehicle and LTA-treated groups, using GraphPad Prism 8. P<0.05 was considered to indicate a statistically significant difference.

Results

Distribution of mRNA expression in human neutrophils following LTA stimulation. Previous publications have reported that stimulation with 0.1-10 μg/ml of *S. aureus* LTA induced the release of cytokines, such as IL-8 and TNF-α, in human monocytes within 1-6 h (38,39). In addition, the

Table I. GO analysis for biological processes via DAVID gene functional classification tool.

GO ID	GO term	Enrichment	P-value	FDR
GO:0030335	Positive regulation of cell migration	6.237193	$6.81x10^{-19}$	$1.29x10^{-15}$
GO:0051272	Positive regulation of cellular component movement	6.020298	$7.20x10^{-19}$	$1.36x10^{-15}$
GO:2000147	Positive regulation of cell motility	6.023695	$2.17x10^{-18}$	$4.11x10^{-15}$
GO:0030334	Regulation of cell migration	4.543111	$2.72x10^{-18}$	$5.16x10^{-15}$
GO:0040017	Positive regulation of locomotion	5.838131	$6.11x10^{-18}$	$1.16x10^{-14}$
GO:2000145	Regulation of cell motility	4.316392	$8.70x10^{-18}$	$1.65x10^{-14}$
GO:0006954	Inflammatory response	4.580108	$2.92x10^{-17}$	$5.54x10^{-14}$
GO:0040012	Regulation of locomotion	4.136543	$4.70x10^{-17}$	$8.90x10^{-14}$
GO:0006952	Defense response	2.989709	$4.85x10^{-17}$	$9.19x10^{-14}$
GO:0051270	Regulation of cellular component movement	4.042019	$5.25x10^{-17}$	$9.93x10^{-14}$
GO:0016477	Cell migration	3.285506	$3.73x10^{-16}$	$6.33x10^{-13}$
GO:0070887	Cellular response to chemical stimulus	2.301508	$9.52x10^{-16}$	$1.89x10^{-12}$
GO:0006950	Response to stress	2.010083	$2.23x10^{-15}$	$4.21x10^{-12}$
GO:0009605	Response to external stimulus	2.502035	$4.33x10^{-15}$	$8.19x10^{-12}$
GO:0051674	Localization of cell	3.022336	$4.56x10^{-15}$	$8.62x10^{-12}$
GO:0048870	Cell motility	3.022336	$4.56x10^{-15}$	$8.62x10^{-12}$
GO:0007166	Cell surface receptor signaling pathway	2.234817	$1.38x10^{-14}$	$2.61x10^{-11}$
GO:0032879	Regulation of localization	2.280856	$3.45x10^{-14}$	$6.54x10^{-11}$
GO:0010033	Response to organic substance	2.159601	$4.98x10^{-14}$	$9.42x10^{-11}$
GO:0048583	Regulation of response to stimulus	1.961424	$6.01x10^{-14}$	$1.14x10^{-10}$

GO, Gene Ontology; FDR, false discovery rate.

gene expression profile of the human monocyte cell line THP-1 following stimulation with 25 μg/ml LTA for 6 h was detected via microarray analysis (40). The results indicated that genes involved in inflammatory responses, cell adhesion, cytokines and chemokines were upregulated following *S. aureus* LTA stimulation (40). In the present study, to investigate the mRNA and miRNA expression changes in human neutrophils, human CD66abce$^+$ cells were enriched from peripheral blood obtained from a healthy donor. In peripheral blood, the majority of the enriched CD66abce$^+$ cells are considered neutrophils (41,42). The purity of the CD66acbe$^+$ cells following enrichment was >98%, as evidenced by flow cytometry analysis (Fig. 1A). Because 1 μg/ml of LTA stimulation has been shown to be sufficient to activate signaling downstream of TLR2 in immune cells (43), and the gene expression profile of LTA-stimulated neutrophils has not been investigated, the isolated human CD66abce$^+$ cells were stimulated with 1 μg/ml LTA from *S. aureus* (LTA group) or vehicle control (ddH2O; Veh group) for 16 h and then the total RNA was extracted. Quality assessment of the RNA sequencing analysis is shown in Figs. S2 and S3, reporting high scores in per-base sequence quality and per-sequence quality in both groups. The mapped reads for both RNA and small RNA sequencing are listed in Table SI. The expression was normalized in FPKM mapped reads. The distribution of the FPKM values of the two samples was presented in a density plot (Fig. 1B). The results suggested that the FPKM distribution was similar in the two samples. To further investigate the differential gene expression in response to LTA stimulation, the distribution of differentially expressed genes between the two samples was plotted in a volcano plot (Fig. 1C). Genes with fold change ≥2.0 (log_2 fold change >1 or <-1), FPKM >0.8 and P-value <0.05 ($-log_{10}$ P-value >1.3) were considered as significant. According to these criteria, 290 significant differentially expressed genes were selected for subsequent analysis (the full gene list is presented in Table SII). Furthermore, the mRNA expression changes of CCL2, CCL7 and CXCL5 were validated by RT-qPCR (Fig. 1D), confirming that these genes were demonstrate to be significantly upregulated following LTA stimulation by both the RT-qPCR and the RNA sequencing analyses.

Evaluating the function of LTA-affected genes. Previous studies have suggested that LTA stimulation results in induction of inflammatory cytokines and chemokines, cell migration and antimicrobial responses in immune cells. To further investigate the function of the differential gene expression in response to LTA stimulation, the 290 selected genes were subjected to GO analysis for biological processes and KEGG pathway analysis via the DAVID gene functional classification tool. Results with P-values <0.001 and FDR <25% were considered as significantly enriched biological processes and KEGG pathways. The results revealed that >200 biological processes and 4 KEGG pathways were enriched. The gene list in each enriched biological process and KEGG pathway is present in Tables SIII and SIV. The top 20 most significant enriched biological processes are presented in Table I. These biological processes, including positive regulation of cell migration and

Table II. Kyoto encyclopedia of genes and genomes pathway analysis via DAVID gene functional classification tool.

Path ID	Path name	Enrichment	P-value	FDR
hsa04060	Cytokine-cytokine receptor interaction	4.2657	2.88×10^{-8}	3.62×10^{-5}
hsa05205	Proteoglycans in cancer	3.5337	7.46×10^{-5}	0.0938
hsa04015	Rap1 signaling pathway	3.3655	1.26×10^{-4}	0.1585
hsa04062	Chemokine signaling pathway	3.5464	1.38×10^{-4}	0.1738

FDR, false discovery rate.

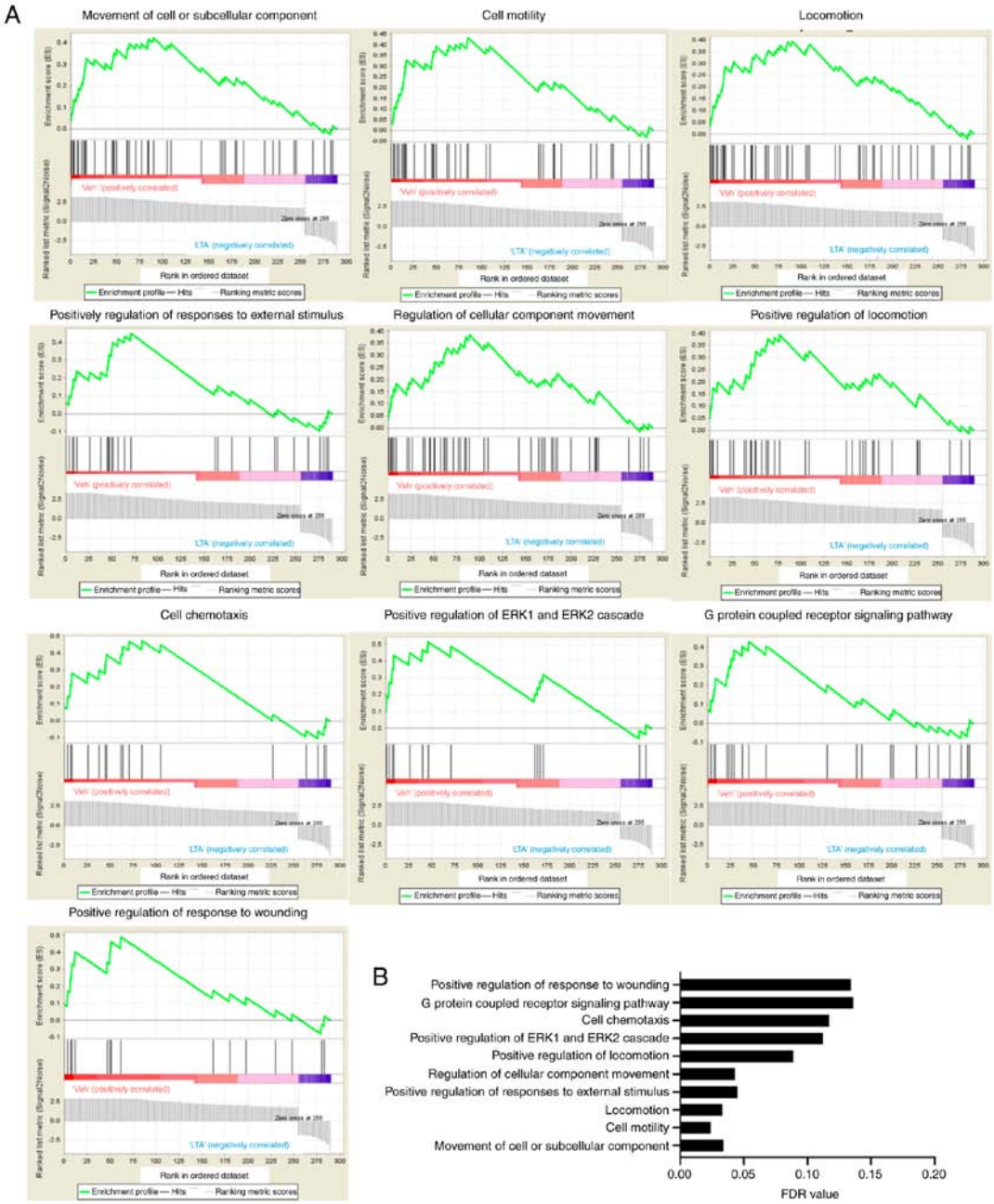

Figure 2. Gene ontology analysis for biological processes via Gene Set Enrichment Analysis. (A) Histograms of selected top enriched signatures. (B) FDR values of the top ten significantly enriched-biological processes. FDR, false discovery rate.

motility, positive regulation of cellular component movement, response to external stimulus, defense responses, inflammatory responses and cell surface receptor signaling pathway, were similar with the LTA-induced responses of

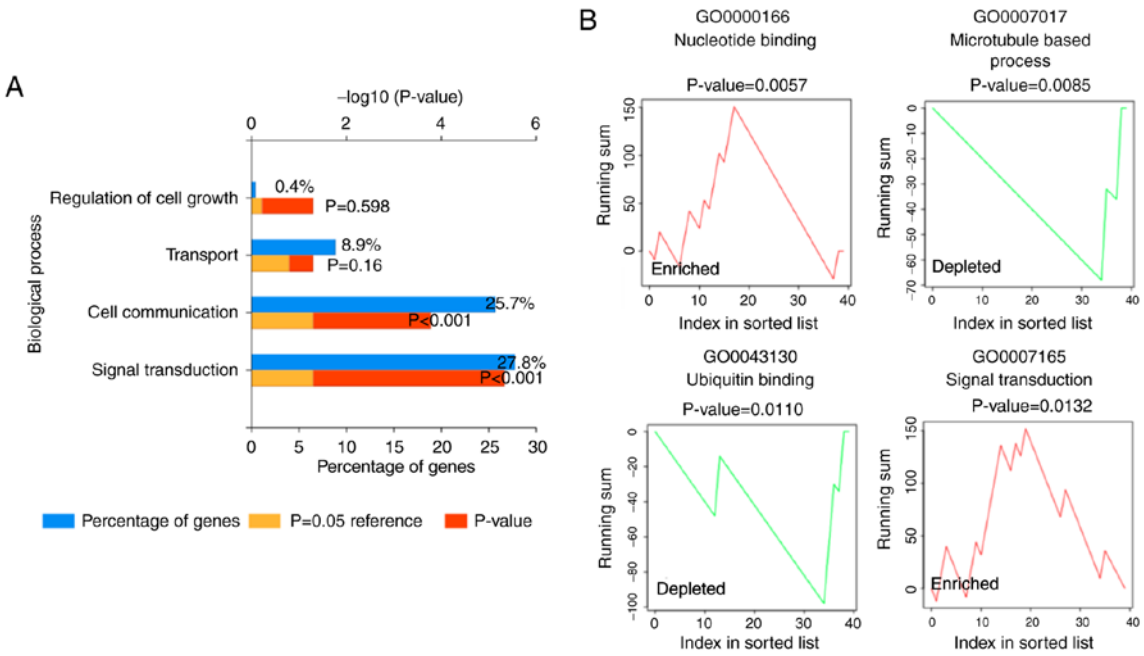

Figure 3. Gene ontology analysis of miRNAs. (A) Enriched biological pathways generated by the Funrich software analysis. (B) Enriched biological pathways generated by the miEAA website. Two enriched (red) and two depleted (green) biological pathways are shown.

neutrophils in previous studies (11-14). The results of KEGG pathway analysis are presented Table II.

The functions of the 290 genes were also analyzed by GSEA. The results revealed that 53 gene sets were significant at FDR <25% and 16 gene sets were significant at nominal P-value <1%. According to the FDR value, the top 10 most significant gene sets are presented in Fig. 2. The gene sets identified by GSEA analysis were similar with those from GO analysis, including cell motility, locomotion, cellular component movement, G protein-coupled receptor signaling and positive regulation of ERK1 and ERK2 cascade, were shown. Upregulation of cell migration and granule degranulation in LTA-stimulated neutrophils has been reported in previous studies (11-14). By contrast, upregulation of cytokines, such as IL-8, IL-6, TNF-α and G-CSF, was not observed in the present results; the expression changes of those four genes were <2-fold in the present RNA sequencing results (data not shown).

Evaluating the function of LTA-affected miRNAs. The miRNA expression was also determined via miRNA sequencing in the present study. miRNA expression was considered significantly changed based on fold change ≥2.0 and reads per million (RPM) >1. Compared to vehicle-stimulated neutrophils, 38 miRNAs, including 36 downregulated miRNAs and 2 upregulated miRNAs, were identified as significantly differentially expressed in LTA-stimulated neutrophils. The list of the 38 significant differentially expressed miRNAs is presented in Table SV. The miRNA enrichment analysis was determined via Funrich software according to biological process. The Funrich analysis suggested that these miRNAs were significantly involved in signal transduction and cell communication (P<0.05; Fig. 3A). In addition, the GSEA-like method of gene ontology analysis was performed via the miEAA website, which is a miRNA enrichment analysis and annotation web-based application. Pathways such as nucleotide binding, signal transduction, cell cortex, protein autophosphorylation, transcription corepressor and energy reserve metabolic process were enriched in the LTA-stimulated neutrophils (Fig. 3B and Table III). Pathways such as microtubule-based process, cytoskeleton-dependent intracellular transport, protein polymerization and ubiquitin binding were suppressed (Fig. 3B and Table III). Signal transduction was the only enriched biological process observed with both the analysis methods.

Evaluating the potential interaction between LTA-affected miRNA and genes. To further identify whether the 38 miRNAs may interact with the 290 LTA-affected genes, the Funrich software and the miRDB website were used. The analysis results of the Funrich software and the miRDB website, respectively, indicated 264 miRNAs and 350 miRNAs might target to 342 genes. Seven and 15 shared miRNAs were respectively identified between the 38 miRNAs and 264 Funrich-predicted miRNAs (Fig. 4A), and 38 miRNAs and 350 miRDB-predicted miRNAs (Fig. 4B). The results further revealed that 5 miRNAs, hsa-miR-1271-5p, hsa-miR-708-5p, hsa-miR-362-3p, hsa-miR-34c-5p and hsa-miR-34a-5p, were observed in both analyses. The potential interaction between 5 miRNAs and 290 genes was further validated by Targetscan and miRTarBase database analyses. The interaction between the 4 miRNAs and the 5 genes is presented in Table IV. These genes were involved in various biological processes. For example, MET proto-oncogene (MET) and heparin binding EGF like growth factor (HBEGF) were involved in positive regulation of cell migration and cellular component movement, calcium voltage-gated channel auxiliary subunit β3 (CACNB3) was involved in immune system process and immune response, tensin 3 (TNS3) was involved in cell migration and motility, and tweety family member 3 (TTYH3) involved in localization (Table SII). The interactions between

Table III. GO analysis of miRNA via miEAA website.

GO ID	Path name	Enrichment	P-value	miRNA
GO0000166	Nucleotide binding	Enriched	0.0057	hsa-miR-10a-3p; hsa-miR-193a-3p; hsa-miR-22-5p; hsa-miR-331-5p; hsa-miR-34a-5p; hsa-miR-34c-5p; hsa-miR-362-5p; hsa-miR-378a-5p; hsa-miR-940
GO0007017	Microtubule based process	Depleted	0.0085	hsa-miR-708-5p; hsa-miR-940
GO0030705	Cytoskeleton dependent intracellular transport	Depleted	0.0085	hsa-miR-708-5p; hsa-miR-940
GO0051258	Protein polymerization	Depleted	0.0085	hsa-miR-708-5p; hsa-miR-940
GO0043130	Ubiquitin binding	Depleted	0.0110	hsa-miR-34a-5p; hsa-miR-708-5p; hsa-miR-708-3p; hsa-miR-940
GO0007165	Signal transduction	Enriched	0.0132	hsa-miR-10a-3p; hsa-miR-1271-5p; hsa-miR-22-5p; hsa-miR-31-3p; hsa-miR-331-5p; hsa-miR-337-3p; hsa-miR-34a-5p; hsa-miR-34c-5p; hsa-miR-378a-5p; hsa-miR-3928-3p; hsa-miR-625-5p; hsa-miR-708-5p
GO0005938	Cell cortex	Enriched	0.0149	hsa-miR-193a-3p; hsa-miR-31-3p; hsa-miR-34a-5p; hsa-miR-34c-5p
GO0046777	Protein autophosphorylation	Enriched	0.0149	hsa-miR-193a-3p; hsa-miR-31-3p; hsa-miR-34a-5p; hsa-miR-34c-5p
GO0003714	Transcription corepressor activity	Enriched	0.0176	hsa-miR-193a-3p; hsa-miR-34a-5p; hsa-miR-34c-5p; hsa-miR-362-3p; hsa-miR-378a-5p
GO0006112	Energy reserve metabolic process	Enriched	0.0176	hsa-miR-10a-3p; hsa-miR-337-3p; hsa-miR-34a-5p; hsa-miR-34c-5p; hsa-miR-378a-5p

GO, Gene Ontology; miRNA, microRNA.

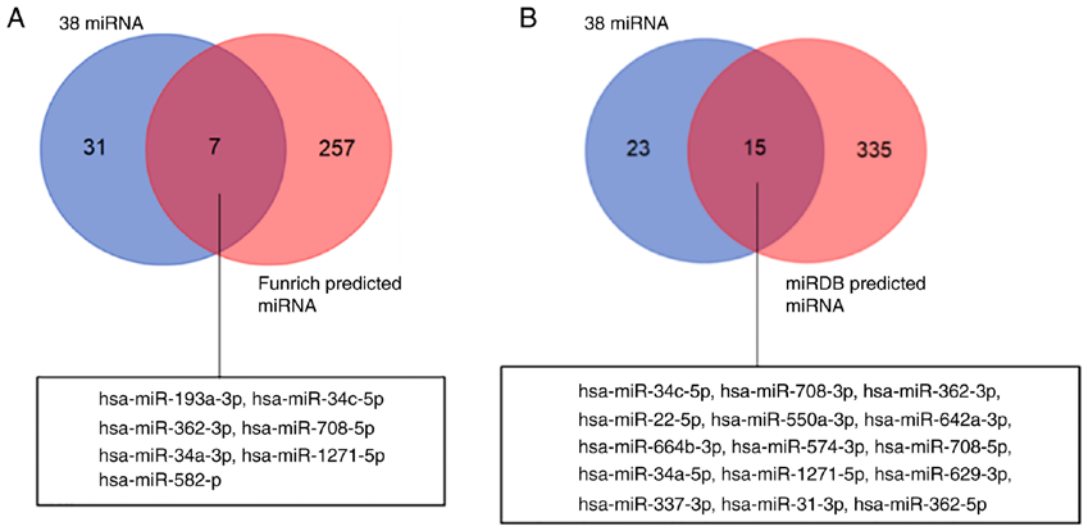

Figure 4. The potential targeted genes of miRNAs. The results of miRNA sequencing revealed that 38 miRNAs exhibited differential expression between lipoteichoic acid and vehicle-stimulated neutrophils. (A) Venn diagram showing that the 7 miRNAs identified in the Funrich software predicted 264 miRNAs (red circle) and 38 miRNAs (blue circle; P=0.262). (B) Venn diagram showing that the 15 miRNAs in the miRDB website predicted 350 miRNAs (red circle) and 38 miRNAs (blue circle; P=0.002).

hsa-miR-34a-5p, hsa-miR-34c-5p and MET, hsa-miR-34a-5p and CACNB3, and their biological function have been validated in other publications (44-52).

Although interactions were predicted between the 4 miRNAs and the 5 genes, potential interactions between most of genes and miRNAs identified in the present study were not identified. Because LTA stimulation induces defense responses, further analysis focused on the genes and miRNAs involved in the biological processes of positive regulation of cell migration and motility and cellular component movement (Fig. 5). The results revealed that various genes with >2-fold changes may also interact with miRNAs with <2-fold changes.

Table IV. Target genes of miRNAs.

miRNA	Fold change of miRNA[a]	Gene symbol	Fold change of mRNA[a]	TargetScan	miRTarBase	(Refs.)
hsa-miR-34a-5p	-2.18	MET	2.23	Yes	Yes	(40,46-48)
hsa-miR-34a-5p	-2.18	CACNB3	0.49	Yes	Yes	(45)
hsa-miR-34c-5p	-2.11	MET	2.23	Yes	Yes	(40-44)
hsa-miR-708-5p	-2.07	TNS3	6.41	Yes	No	
hsa-miR-1271-5p	-2.98	TTYH3	2.70	Yes	No	
hsa-miR-1271-5p	-2.98	TNS3	6.41	Yes	No	
hsa-miR-1271-5p	-2.98	HBEGF	3.78	Yes	No	

[a]Fold change in lipoteichoic acid-treated group vs. vehicle group. MET, MET proto-oncogene; CACNB3, calcium voltage-gated channel auxiliary subunit β3; TNS3, tensin 3; TTYH3, tweety family member 3; HBEGF, heparin binding EGF like growth factor.

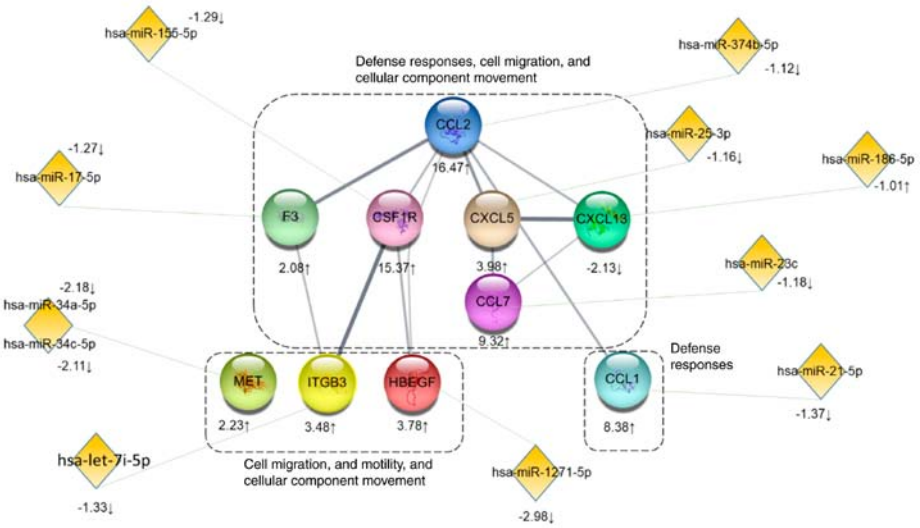

Figure 5. Interactions of miRNAs and genes. The genes involved in the biological processes 'defense responses', 'positive regulation of cell migration and mobility' and 'positive regulation of cellular component movement' were selected and potential targeted miRNAs were predicted by the Funrich software and the miRDB website (target score >90). The circles represent genes and the diamonds represent miRNAs. The numbers beside the genes and the miRNAs indicate fold changes. The green lines linking between genes and miRNAs indicate potential interactions.

Further experimental evidence will be necessary to confirm whether miRNA-mRNA interactions may be important for regulation of LTA-induced signaling pathways.

Discussion

LTA is a cell wall polymer in Gram-positive bacteria and a risk factor for sepsis. Based on their chemical structures, LTAs can be grouped into different types. Type I LTA is present in bacteria including *S. aureus*, *Listeria monocytogenes* and *Bacillus subtilis* (53). Prior publications have reported that LTAs from *S. aureus* and *Streptococcus pneumoniae* (type IV) can induce secretion of IL-8, IL-6, IL-1β and TNF-α in monocytes and macrophages (54,55). Although the half-life of circulating neutrophils is only 6-8 h (56), a previous study demonstrated that the production of IL-1β, IL-8 and TNF-α was significantly induced when human neutrophils were incubated with 10 μg/ml *S. aureus* LTA for 16 and 24 h (14). In addition, Hattar *et al* (14) demonstrated that the protein levels of IL-8 were induced by stimulation with 1, 5 and 10 μg/ml LTA after 16 h of incubation. In the present study, the results of RNA sequencing provided a whole molecular picture of LTA-induced gene expression, including a trend for increased expression of IL-8, IL-6, TNF-α and G-CSF (although <2-fold), and 290 genes with significantly differential expression in human neutrophils following 16 h stimulation with 1 μg/ml LTA.

LTA-affected genes have been reported in several types of cells in previous studies. Two previously published datasets in the Gene Expression Omnibus (GEO) database, GSE15512 and GSE21188, include results from microarray analysis determining the gene expression of an LTA-treated monocyte cell line (25 μg/ml LTA was used to stimulate THP-1 cells for 6 h) and peripheral blood mononuclear cells (PBMCs; 10 μg/ml LTA was used to stimulate PBMCs for 7 h), respectively. Although the dose and duration of the LTA stimulations were not identical, the expression of inflammatory genes in the present study was compared with that in both datasets. In

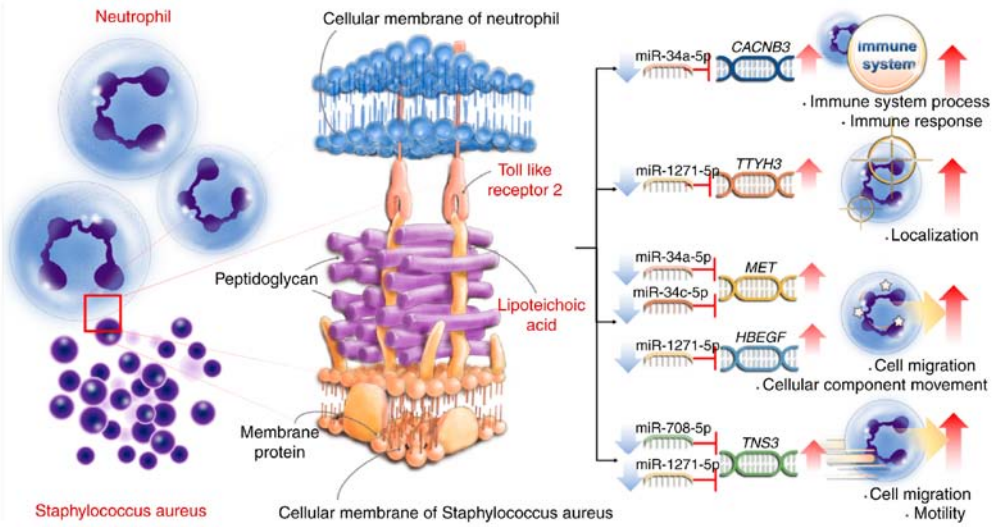

Figure 6. Schematic summary of proposed miRNA-target gene interactions and biological processes in human neutrophils following lipoteichoic acid stimulation. CACNB3, calcium voltage-gated channel auxiliary subunit β3; TTYH3, tweety family member 3; MET, MET proto-oncogene; HBEGF, heparin binding EGF like growth factor; TNS3, tensin 3.

general, the upregulated expression of genes including IL-1β, IL-6, CXCL8, CCL2 and CCL20 were similar in the present study and both datasets. Notably, LTA stimulation in THP-1 cells induced more significant changes in gene expression compared with LTA stimulation in PBMCs and in the present study. Based on 20 shared inflammatory-associated genes among the present study and the two public databases, the gene expression profile in the present study was moderately positively correlated with that in the public databases. These findings might suggest that genes can be affected differently by the various doses of LTA in a short (6-7 h) and long (16 h) incubation period.

The results of mRNA sequencing revealed various biological processes and signaling pathways that were enriched following LTA stimulation. In Table I, positively regulation of cell migration, cell motility and locomotion, as well as defense responses and inflammatory responses, were observed. Additionally, KEGG pathway analysis revealed that 4 pathways were enriched, including cytokine-cytokine receptor interaction and chemokine signaling pathway (Table II). A previous study demonstrated that *B. subtilis* LTA increases the secretion of CCL2 and CXCL10 in odontoblasts (57). To the best of our knowledge, the induction of chemokines is not fully elucidated in neutrophils. In odontoblasts, fibroblasts and pulpal cells, activation of TLR2, TLR3 and TLR4 pathways induces the production of several chemokines, such as CCL2, CCL7, IL-8 (CXCL8) and CXCL10 (58,59). In human lymphatic endothelium cells, LTA stimulation induces the expression of CCL2, CCL5, CXCL1, CXCL3, CXCL5, CXCL6 and IL-8 (CXCL8) through a TLR2-depedent mechanism (60). The present study revealed upregulation of CCL2, CCL7 and CXCL5 in LTA-stimulated neutrophils (Fig. 5). In addition, the expression of TLR2 was also upregulated (by 2.02-fold) following LTA stimulation. Therefore, it is supposed that TLR2 might be also essential for chemokine signaling pathway in human neutrophils. The role of TLR2 in the regulation of the chemokine signaling pathway, the function of proteoglycans, and the role of the Rap1 signaling pathway in neutrophils, will be further investigated in subsequent studies.

The effect of LTA stimulation on the miRNA expression remained unclear. In a mouse model, *Staphylococcus epidermidis* LTA induced the expression of miR-143 via TLR2 signaling (61). When mice were exposed to LTA from *B. subtilis*, *S. faecalis* and *S. aureus*, the expression of miR-451, miR-668, miR-1902 and miR-1904 was induced in whole blood and serum (62). The present study found 38 miRNAs with >2-fold change in expression following LTA stimulation; the majority of these 38 miRNAs were novel and not reported in previous publications. However, miR-143, miR-451, miR-668, miR-1902 and miR-1904 were not significantly altered in the human LTA-stimulated neutrophils in the present study. Because a miRNA can target many genes (63), GO analysis of the 38 miRNAs was performed (Table III). However, the function of these miRNAs and the regulatory mechanism of these enriched biological processes and LTA-mediated responses remained unknown. Therefore, the miRNA-target gene interactions were further investigated via multiple bioinformatic tools. The results revealed potential novel interactions between hsa-miR-34a-5p, hsa-miR-34c-5p, hsa-miR-708-5p hsa-miR-1271-5p and MET, HBEGF, CACNB3, TNS3 and TTYH3, and that these interactions may regulate cell migration and motility, cellular component movement, immune system process and immune response. Although these findings were interesting, there are some limitations in the current study. Firstly, only one sample from one donor was analyzed in the present study. Furthermore, the interactions between miRNA and mRNA were not experimentally confirmed. The proposed interactions require further validation through functional experiments in the future. The summary of the present findings is presented in Fig. 6.

To the best of our knowledge, the present study is the first to provide comprehensive information about transcriptome analysis of LTA-stimulated human neutrophils. A total of 290 mRNAs and 38 miRNAs which were significantly altered by 16 h-stimulation of *S. aureus* LTA in human neutrophils were

identified. Furthermore, bioinformatic analysis proposed novel interactions between 4 miRNAs and 5 target genes. These findings may provide new insights of the LTA-mediated effect on peripheral neutrophils and the innate immune responses in a healthy person.

Acknowledgements

The authors thank the Center for Research Resources and Development of Kaohsiung Medical University.

Funding

This study was supported by grants from the Ministry of Science and Technology (grant nos. MOST 108-2314-B-037-097-MY3, 107-2320-B-037-011-MY3 and 106-2320-B-037-029-MY3), the Kaohsiung Medical University Hospital (grant nos. KMUH107-7M36, KMUH107-7R81, KMUHS10701 and KMUHS10712), the Kaohsiung Medical University Research Center Grant (grant no. KMU-TC108A04) and the Kaohsiung Medical University (grant nos. KMU-DK108003 and KMU-Q108005).

Availability of data and materials

The datasets used and/or analyzed during the current study are available from the corresponding author on reasonable request.

Authors' contributions

MY and MT conceived and designed the experiments. IY, KL and SJ prepared the materials and performed the experiments. MY, IY, CL, MT and PK analyzed the data. MY wrote the manuscript. All authors read and approved the final manuscript.

Ethics approval and consent to participate

This study was approved by the Institutional Review Board of Kaohsiung Medical University Hospital (IRB no. KMUH-IRB-20120287). Signed informed consent was obtained.

Patient consent for publication

Not applicable.

Competing interests

The authors declare that they have no competing interests.

References

1. Brubaker SW, Bonham KS, Zanoni I and Kagan JC: Innate immune pattern recognition: A cell biological perspective. Annu Rev Immunol 33: 257-290, 2015.
2. Mogensen TH: Pathogen recognition and inflammatory signaling in innate immune defenses. Clin Microbiol Rev 22: 240-273, Table of Contents, 2009.
3. Kawasaki T and Kawai T: Toll-like receptor signaling pathways. Front Immunol 5: 461, 2014.
4. Lu YC, Yeh WC and Ohashi PS: LPS/TLR4 signal transduction pathway. Cytokine 42: 145-151, 2008.
5. Park BS and Lee JO: Recognition of lipopolysaccharide pattern by TLR4 complexes. Exp Mol Med 45: e66, 2013.
6. Seo HS, Michalek SM and Nahm MH: Lipoteichoic acid is important in innate immune responses to gram-positive bacteria. Infect Immun 76: 206-213, 2008.
7. Schwandner R, Dziarski R, Wesche H, Rothe M and Kirschning CJ: Peptidoglycan- and lipoteichoic acid-induced cell activation is mediated by toll-like receptor 2. J Biol Chem 274: 17406-17409, 1999.
8. Oliveira-Nascimento L, Massari P and Wetzler LM: The role of TLR2 in infection and immunity. Front Immunol 3: 79, 2012.
9. Kengatharan KM, De Kimpe S, Robson C, Foster SJ and Thiemermann C: Mechanism of gram-positive shock: Identification of peptidoglycan and lipoteichoic acid moieties essential in the induction of nitric oxide synthase, shock, and multiple organ failure. J Exp Med 188: 305-315, 1998.
10. Kurt-Jones EA, Mandell L, Whitney C, Padgett A, Gosselin K, Newburger PE and Finberg RW: Role of toll-like receptor 2 (TLR2) in neutrophil activation: GM-CSF enhances TLR2 expression and TLR2-mediated interleukin 8 responses in neutrophils. Blood 100: 1860-1868, 2002.
11. Lotz S, Aga E, Wilde I, van Zandbergen G, Hartung T, Solbach W and Laskay T: Highly purified lipoteichoic acid activates neutrophil granulocytes and delays their spontaneous apoptosis via CD14 and TLR2. J Leukoc Biol 75: 467-477, 2004.
12. Ginsburg I: Role of lipoteichoic acid in infection and inflammation. Lancet Infect Dis 2: 171-179, 2002.
13. Nathan C: Neutrophils and immunity: Challenges and opportunities. Nat Rev Immunol 6: 173-182, 2006.
14. Hattar K, Grandel U, Moeller A, Fink L, Iglhaut J, Hartung T, Morath S, Seeger W, Grimminger F and Sibelius U: Lipoteichoic acid (LTA) from *Staphylococcus aureus* stimulates human neutrophil cytokine release by a CD14-dependent, Toll-like-receptor-independent mechanism: Autocrine role of tumor necrosis factor-[alpha] in mediating LTA-induced interleukin-8 generation. Crit Care Med 34: 835-841, 2006.
15. Drury RE, O'Connor D and Pollard AJ: The clinical application of MicroRNAs in infectious disease. Front Immunol 8: 1182, 2017.
16. Liu H, Lei C, He Q, Pan Z, Xiao D and Tao Y: Nuclear functions of mammalian MicroRNAs in gene regulation, immunity and cancer. Mol Cancer 17: 64, 2018.
17. Wen Z, Xu L, Chen X, Xu W, Yin Z, Gao X and Xiong S: Autoantibody induction by DNA-containing immune complexes requires HMGB1 with the TLR2/microRNA-155 pathway. J Immunol 190: 5411-5422, 2013.
18. Yao H, Zhang H, Lan K, Wang H, Su Y, Li D, Song Z, Cui F, Yin Y and Zhang X: Purified *Streptococcus pneumoniae* endopeptidase O (PepO) enhances particle uptake by macrophages in a toll-like receptor 2- and miR-155-dependent manner. Infect Immun 85: e01012-e01016, 2017.
19. Xu H, Wu Y, Li L, Yuan W, Zhang D, Yan Q, Guo Z and Huang W: MiR-344b-1-3p targets TLR2 and negatively regulates TLR2 signaling pathway. Int J Chron Obstruct Pulmon Dis 12: 627-638, 2017.
20. Landais I, Pelton C, Streblow D, DeFilippis V, McWeeney S and Nelson JA: Human cytomegalovirus miR-UL112-3p targets TLR2 and modulates the TLR2/IRAK1/NFκB signaling pathway. PLoS Pathog 11: e1004881, 2015.
21. Quinn EM, Wang JH, O'Callaghan G and Redmond HP: MicroRNA-146a is upregulated by and negatively regulates TLR2 signaling. PLoS One 8: e62232, 2013.
22. Bolger AM, Lohse M and Usadel B: Trimmomatic: A flexible trimmer for Illumina sequence data. Bioinformatics 30: 2114-2120, 2014.
23. Kim D, Langmead B and Salzberg SL: HISAT: A fast spliced aligner with low memory requirements. Nat Methods 12: 357-360, 2015.
24. Friedlander MR, Mackowiak SD, Li N, Chen W and Rajewsky N: miRDeep2 accurately identifies known and hundreds of novel microRNA genes in seven animal clades. Nucleic Acids Res 40: 37-52, 2012.
25. Trapnell C, Roberts A, Goff L, Pertea G, Kim D, Kelley DR, Pimentel H, Salzberg SL, Rinn JL and Pachter L: Differential gene and transcript expression analysis of RNA-seq experiments with TopHat and cufflinks. Nat Protoc 7: 562-578, 2012.
26. Livak KJ and Schmittgen TD: Analysis of relative gene expression data using real-time quantitative PCR and the 2(-Delta Delta C(T)) method. Methods 25: 402-408, 2001.

27. Huang da W, Sherman BT and Lempicki RA: Systematic and integrative analysis of large gene lists using DAVID bioinformatics resources. Nat Protoc 4: 44-57, 2009.
28. Huang da W, Sherman BT and Lempicki RA: Bioinformatics enrichment tools: Paths toward the comprehensive functional analysis of large gene lists. Nucleic Acids Res 37: 1-13, 2009.
29. Subramanian A, Tamayo P, Mootha VK, Mukherjee S, Ebert BL, Gillette MA, Paulovich A, Pomeroy SL, Golub TR, Lander ES and Mesirov JP: Gene set enrichment analysis: A knowledge-based approach for interpreting genome-wide expression profiles. Proc Natl Acad Sci USA 102: 15545-15550, 2005.
30. Mootha VK, Lindgren CM, Eriksson KF, Subramanian A, Sihag S, Lehar J, Puigserver P, Carlsson E, Ridderstråle M, Laurila E, *et al*: PGC-1alpha-responsive genes involved in oxidative phosphorylation are coordinately downregulated in human diabetes. Nat Genet 34: 267-273, 2003.
31. Backes C, Khaleeq QT, Meese E and Keller A: miEAA: microRNA enrichment analysis and annotation. Nucleic Acids Res 44: W110-W116, 2016.
32. Pathan M, Keerthikumar S, Ang CS, Gangoda L, Quek CY, Williamson NA, Mouradov D, Sieber OM, Simpson RJ, Salim A, *et al*: FunRich: An open access standalone functional enrichment and interaction network analysis tool. Proteomics 15: 2597-2601, 2015.
33. Liu W and Wang X: Prediction of functional microRNA targets by integrative modeling of microRNA binding and target expression data. Genome Biol 20: 18, 2019.
34. Garcia DM, Baek D, Shin C, Bell GW, Grimson A and Bartel DP: Weak seed-pairing stability and high target-site abundance decrease the proficiency of lsy-6 and other microRNAs. Nat Struct Mol Biol 18: 1139-1146, 2011.
35. Chou CH, Shrestha S, Yang CD, Chang NW, Lin YL, Liao KW, Huang WC, Sun TH, Tu SJ, Lee WH, *et al*: miRTarBase update 2018: A resource for experimentally validated microRNA-target interactions. Nucleic Acids Res 46: D296-D302, 2018.
36. Shannon P, Markiel A, Ozier O, Baliga NS, Wang JT, Ramage D, Amin N, Schwikowski B and Ideker T: Cytoscape: A software environment for integrated models of biomolecular interaction networks. Genome Res 13: 2498-2504, 2003.
37. Doncheva NT, Morris JH, Gorodkin J and Jensen LJ: Cytoscape stringApp: Network analysis and visualization of proteomics data. J Proteome Res 18: 623-632, 2019.
38. Finney SJ, Leaver SK, Evans TW and Burke-Gaffney A: Differences in lipopolysaccharide- and lipoteichoic acid-induced cytokine/chemokine expression. Intensive Care Med 38: 324-332, 2012.
39. Schröder NW, Morath S, Alexander C, Hamann L, Hartung T, Zähringer U, Göbel UB, Weber JR and Schumann RR: Lipoteichoic acid (LTA) of *Streptococcus pneumoniae* and *Staphylococcus aureus* activates immune cells via Toll-like receptor (TLR)-2, lipopolysaccharide-binding protein (LBP), and CD14, whereas TLR-4 and MD-2 are not involved. J Biol Chem 278: 15587-15594, 2003.
40. Zeng RZ, Kim HG, Kim NR, Gim MG, Ko MY, Lee SY, Kim CM and Chung DK: Differential gene expression profiles in human THP-1 monocytes treated with *Lactobacillus plantarum* or *Staphylococcus aureus* lipoteichoic acid. J Korean Soc Appl Bi 54: 763-770, 2011.
41. Sharma S, Davis RE, Srivastva S, Nylen S, Sundar S and Wilson ME: A subset of neutrophils expressing markers of antigen-presenting cells in human visceral leishmaniasis. J Infect Dis 214: 1531-1538, 2016.
42. Chen X, Li SJ, Ojcius DM, Sun AH, Hu WL, Lin X and Yan J: Mononuclear-macrophages but not neutrophils act as major infiltrating anti-leptospiral phagocytes during leptospirosis. PLoS One 12: e0181014, 2017.
43. Long EM, Millen B, Kubes P and Robbins SM: Lipoteichoic acid induces unique inflammatory responses when compared to other toll-like receptor 2 ligands. PLoS One 4: e5601, 2009.
44. Hermeking H: The miR-34 family in cancer and apoptosis. Cell Death Differ 17: 193-199, 2010.
45. Cai KM, Bao XL, Kong XH, Jinag W, Mao MR, Chu JS, Huang YJ and Zhao XJ: Hsa-miR-34c suppresses growth and invasion of human laryngeal carcinoma cells via targeting c-Met. Int J Mol Med 25: 565-571, 2010.
46. Dong F and Lou D: MicroRNA-34b/c suppresses uveal melanoma cell proliferation and migration through multiple targets. Mol Vis 18: 537-546, 2012.
47. Hagman Z, Haflidadottir BS, Ansari M, Persson M, Bjartell A, Edsjö A and Ceder Y: The tumour suppressor miR-34c targets MET in prostate cancer cells. Br J Cancer 109: 1271-1278, 2013.
48. Wang F, Lu J, Peng X, Wang J, Liu X, Chen X, Jiang Y, Li X and Zhang B: Integrated analysis of microRNA regulatory network in nasopharyngeal carcinoma with deep sequencing. J Exp Clin Cancer Res 35: 17, 2016.
49. Bavamian S, Mellios N, Lalonde J, Fass DM, Wang J, Sheridan SD, Madison JM, Zhou F, Rueckert EH, Barker D, *et al*: Dysregulation of miR-34a links neuronal development to genetic risk factors for bipolar disorder. Mol Psychiatry 20: 573-584, 2015.
50. Yan D, Zhou X, Chen X, Hu DN, Dong XD, Wang J, Lu F, Tu L and Qu J: MicroRNA-34a inhibits uveal melanoma cell proliferation and migration through downregulation of c-Met. Invest Ophthalmol Vis Sci 50: 1559-1565, 2009.
51. Li Y, Guessous F, Zhang Y, Dipierro C, Kefas B, Johnson E, Marcinkiewicz L, Jiang J, Yang Y, Schmittgen TD, *et al*: MicroRNA-34a inhibits glioblastoma growth by targeting multiple oncogenes. Cancer Res 69: 7569-7576, 2009.
52. Yan K, Gao J, Yang T, Ma Q, Qiu X, Fan Q and Ma B: MicroRNA-34a inhibits the proliferation and metastasis of osteosarcoma cells both in vitro and in vivo. PLoS One 7: e33778, 2012.
53. Percy MG and Grundling A: Lipoteichoic acid synthesis and function in gram-positive bacteria. Annu Rev Microbiol 68: 81-100, 2014.
54. Standiford TJ, Arenberg DA, Danforth JM, Kunkel SL, VanOtteren GM and Strieter RM: Lipoteichoic acid induces secretion of interleukin-8 from human blood monocytes: A cellular and molecular analysis. Infect Immun 62: 119-125, 1994.
55. Mattsson E, Verhage L, Rollof J, Fleer A, Verhoef J and van Dijk H: Peptidoglycan and teichoic acid from *Staphylococcus epidermidis* stimulate human monocytes to release tumour necrosis factor-alpha, interleukin-1 beta and interleukin-6. FEMS Immunol Med Microbiol 7: 281-287, 1993.
56. Summers C, Rankin SM, Condliffe AM, Singh N, Peters AM and Chilvers ER: Neutrophil kinetics in health and disease. Trends Immunol 31: 318-324, 2010.
57. Durand SH, Flacher V, Roméas A, Carrouel F, Colomb E, Vincent C, Magloire H, Couble ML, Bleicher F, Staquet MJ, *et al*: Lipoteichoic acid increases TLR and functional chemokine expression while reducing dentin formation in in vitro differentiated human odontoblasts. J Immunol 176: 2880-2887, 2006.
58. Park C, Lee SY, Kim HJ, Park K, Kim JS and Lee SJ: Synergy of TLR2 and H1R on Cox-2 activation in pulpal cells. J Dent Res 89: 180-185, 2010.
59. Staquet MJ, Durand SH, Colomb E, Roméas A, Vincent C, Bleicher F, Lebecque S and Farges JC: Different roles of odontoblasts and fibroblasts in immunity. J Dent Res 87: 256-261, 2008.
60. Sawa Y, Tsuruga E, Iwasawa K, Ishikawa H and Yoshida S: Leukocyte adhesion molecule and chemokine production through lipoteichoic acid recognition by toll-like receptor 2 in cultured human lymphatic endothelium. Cell Tissue Res 333: 237-252, 2008.
61. Xia X, Li Z, Liu K, Wu Y, Jiang D and Lai Y: Staphylococcal LTA-induced miR-143 inhibits propionibacterium acnes-mediated inflammatory response in skin. J Invest Dermatol 136: 621-630, 2016.
62. Hsieh CH, Yang JC, Jeng JC, Chen YC, Lu TH, Tzeng SL, Wu YC, Wu CJ and Rau CS: Circulating microRNA signatures in mice exposed to lipoteichoic acid. J Biomed Sci 20: 2, 2013.
63. Bartel DP: MicroRNAs: Target recognition and regulatory functions. Cell 136: 215-233, 2009.